THESIS

This is to certify that the

thesis entitled
Characterization of Selective Light Attenuation
by Periphyton

presented by

Richard Frederick Losee

has been accepted towards fulfillment
of the requirements for

M.Sc. degree in Botany

Major professor

Date 2 November 1983

CHARACTERIZATION OF SELECTIVE LIGHT ATTENUATION BY PERIPHYTON

By

Richard Frederick Losee

A THESIS

Submitted to
Michigan State University
in partial fulfillment of the requirements
for the degree of

MASTER OF SCIENCE

Department of Botany and Plant Pathology

1983

ABSTRACT

CHARACTERIZATION OF SELECTIVE LIGHT ATTENUATION BY PERIPHYTON

BY

RICHARD FREDERICK LOSEE

Aquatic habitats are often low-light environments as a consequence of water column selective light attenuation. Periphyton, which consists of algae, bacteria, carbonate crystals, and particulate detritus embedded in a mucoid matrix, exhibits great heterogeneity in three-dimensional geometry and, therefore, contributes to selective light attenuation in a complex manner.

Measures of settled periphyton component absorbances over 10-nm wavebands from 400 to 750 nm showed that algal photosynthetic pigments, particullarly chlorophyll a which absorbs light of the wavelengths submersed macrophytes utilize most efficiently for photosynthesis, dominated light attenuation. Diatom frustules, bacteria, and calcium carbonate crystals contributed very little to selective light attenuation. Three-dimensional community geometry and distribution of absorbing substance effects on light attenuation were investigated by comparing absorbance with the distribution in thickness of settled algae. The severity of periphyton light attenuaiton is a function of community components present, component geometry, and distribution of components within the community.

ACKNOWLEDGMENTS

I wish to acknowledge and thank Dr. Robert G. Wetzel for his encouragement, support and enthusiastic sharing of time and knowledge. The presence of Drs. M.F. Coveney and R.E. Moeller in the laboratory was invaluable because of their willingness to share research experience with a beginner and their participation in stimulating discussion. My colleagues J.M. Burkholder, R.G. Carlton, and W.D. Taylor were always available to assist in activities ranging from manuscript proofing to photographic development. The technical assistance of Dr. F.C. Payne, who provided the spectroradiometer, is gratefully acknowledged. Anita Johnson provided great assistance in preparation of figures, and Jay Sonnad provided much technical assistance. Thanks also to my examination committee members Drs. R.G. Wetzel (Chairman), M.J. Klug, D. Goldberg, and D. Hart for their criticisms and suggestions.

Financial support was provided by the Department of Energy (DE-AC02-76EV01599, C00-1599-239).

TABLE OF CONTENTS

LIST OF TABLES

LIST OF FIGURES

INTRODUCTION

Littoral region influence on lake ecosystem productivity and metabolism is primarily a function of the extent of littoral development and, therefore, is mainly a function of lake basin morphometry. Since most lakes of the world are shallow and of small area, the littoral region is important in most lake ecosystems. The juxtaposition of water, nutrient-rich sediments, and light can result in high primary production in the littoral region, and may contribute significantly to whole lake primary productivity. The littoral region is an interface zone between the land of the drainage basin and the pelagic region. The littoral can moderate fluctuations in, as well as trap, organic and inorganic inputs of influent water. Littoral vegetation is also an ecologically prominent characteristic of lakes, forming habitat for aquatic vertebrates and invertebrates, and substrata for epiphytic fauna and flora.

Zonation of aquatic macrophytes is primarily dependent on light, wave action, sediment type, and temperature (Spence, 1976, 1981, 1982; Barko and Smart, 1981; Barko, 1982). Freshwater environments have been considered low-light (shade) habitats (Spence, 1976), because light is rapidly extinguished with depth as the result of selective attenuation by the molecular characteristics of water, suspended particulate matter, and dissolved organic matter. Selective light attenuation by these components of lake water have been investigated in detail (e.g. reviews

of Hutchinson, 1957; Wetzel, 1983). For example, in natural waters absorption of light in the red wavelengths is usually dominated by pure water absorption while suspended particulate matter absorption is generally nonselective (with the exception of very dense planktonic algal absorption). Absorption by dissolved organic matter is selective and dominates in the ultraviolet, blue, and green wavelengths. As a result of this light attenuation, light availability is often the dominant factor influencing macrophyte distribution.

Sparse macrophyte populations have been observed in association with dense phytoplankton populations in nutrient-enriched waters. Morgan (1970) observed that the macrophyte decline which occurred in Loch Leven coincided with eutrophication of the lake. Experimental fertilization studies (Mulligan and Baranowski, 1969; Moss, 1976) and studies of lakes with varying nutrient levels (Spence, 1976) have established a negative correlation between macrophyte growth and nutrient enrichment of the water column, leading several authors to conclude that submersed macrophyte demise is a result of phytoplankton shading (Olsen, 1964 cited in Morgan, 1970; Moss 1976; Jupp and Spence, 1977). These authors have not considered the effects on macrophyte survival of anoxic, highly reduced sediments which have been shown to decrease macrophyte growth (Mendelssohn, 1981). However, sediment toxicity is primarily mediated by levels of oxygen within the rhizosphere and, therefore, is related to the degree of light attenuation and concomitant photosynthetic oxygen production.

Decreasing growth, photosynthetic rates, abundance, and occurrence of submerged macrophytes have also been attributed to light attenuation by the epiphytic complex (Sand-Jensen, 1977; Eminson and Phillips, 1978;

Phillips et al., 1978; Sand-Jensen and Søndergaard, 1981). Phillips et al. hypothesized that, in progressively eutrophicated waters, phytoplankton populations are maintained at low density through nutrient competition and suppression by organic inhibitors from macrophytes. As eutrophication progresses, epiphytic development increases, hampering submersed macrophyte ability to photosynthesize sufficiently, and may result in a shift in community composition to include more shade-tolerant species or the loss of submersed macrophytes altogether. Phillips et al. (1978) proposed that phytoplankton densities drastically increase only after the submersed macrophyte populations are greatly reduced, thereby relieving phytoplankton from macrophyte nutrient competition and organic-inhibitor suppression.

Evidence for this hypothesis was drawn from the paleolimnological history of the Norfolk Broads (Osborne and Moss, 1977; Phillips et al. 1978). Increasing abundance of epiphytic diatoms in sediments of the Broads coincided with agricultural development of the watershed and resultant increased phosphorus loading. The dense submersed macrophyte beds served as abundant substrata for epiphytic algae. As submersed macrophytes declined, the abundance of planktonic diatoms in the sediments greatly increased. A similar pattern was indicated from laboratory experiments in which submersed plants exposed to higher nutrient treatments grew more slowly and were associated with greater epiphyte density than those exposed to lower nutrient conditions (Eminson and Phillips, 1978). Although greater suspended pigment levels were found in the enriched treatments, these were a result of suspended epiphytic algal clumps rather than a distinct phytoplankton community and did not significantly decrease light available for macrophyte photosynthesis.

The intensity and spectral composition of the light available to submersed macrophytes is modified by selective light attenuation by the components of the water column previously mentioned and the components of the epiphytic complex. The excellent scanning electron micrographs of Allanson (1973) illustrate that periphyton consists of algae (primarily diatoms), bacteria, calcium carbonate crystals, and particulate detritus embedded in a mucoid matrix. The composition and relative distribution of components in this optically complex conglomeration determines the selective light attenuation characteristics of periphyton. Geometry and distribution of scattering surfaces and absorbing material, such as photosynthetic pigments, in the periphyton complex, result in myriad scattering and absorbing interactions. Within the periphyton complex, the major effects of scattering (reflection, refraction, and diffraction) are the remission of light out of the complex, and an increase in pathlength which thereby increases probability of absorption. The selective attenuation characteristics of periphyton components have not previously been examined; therefore, selective attenuation by individual periphyton components was investigated in the present study.

Selective attenuation of radiation between 400 and 750 nm, which includes photosynthetically active radiation (PAR, radiation between 400 and 700 nm), was investigated for individual periphyton components. Living periphyton components included algal species from three divisions and mixed epiphytic bacteria. Nonliving components included bleached green algal cells, acid-cleaned diatom frustules, and calcium carbonate crystals. The nature of light attenuation by communities of varying composition and densities was assessed by measuring the absorption of

single component layers of different densities and comparing the changes in absorbance with changes in density and distributions of material thicknesses. The Lambert-Beer relationship predicts a constant increase in light absorbance with increase in density of a homogeneous distribution of absorbing materials. As the density of layered material is increased, deviation of absorbance spectra from the Lambert-Beer relationship implies there has been an alteration in the distribution and/or composition of absorbing material and, by inference, may be used to characterize the nature of the component effects on attenuation in the periphyton.

MATERIALS AND METHODS

Algae used in this study (Anabaena flos-aquae (Lyngb.) De Bréb., UTEX 1444; Scenedesmus; Navicula pelliculosa (Bréb.) Hilse, UTEX 674; Fragilaria crotonensis Kitton) were grown in axenic culture at 24°C with a 16/8 hour light/dark cycle and 350 $\mu E\ m^{-2}\ s^{-1}$ PAR, supplied by Luxor Vita Lite fluorescent lights, which approximate the daylight spectrum. Cultures were grown on a rotary shaker table (New Brunswick Co.) providing moderate turbulance (about 100 rpm) to cultures. Information pertaining to the preparation and nutrient content of the culture medium used is supplied in Appendix A. The isolation procedure for the epiphytic Scenedesmus is discussed in Appendix B. Bacteria were obtained by inoculating Difco peptone nutrient broth with a 20-ml suspension of material from aerated, decaying submersed macorphytes. The culture was incubated at 25°C and low light (< 5 $\mu E\ m^{-2}\ s^{-1}$ PAR) for three days before concentrating by centrifugation and rinsing with tap water.

Acid-cleaned N. pelliculosa and F. crotonensis frustules were prepared by boiling centrifuged monoalgal suspensions in concentrated nitric acid-potassium dichromate solutions until all organic matter was digested. Cleaned frustules were rinsed copiously with ultrapure (Millipore Q) distilled water. Scenedesmus cells were treated with approximately 2.5% sodium hypochlorite for five seconds and immediately rinsed with distilled water. This oxidative treatment resulted in cells which appeared virtually free of pigment under microscopic examination but with cell walls and ornamentation intact. The calcium carbonate samples were precipitated from saturated solutions of CO_2-$CaCO_3$ distilled water by bubbling with nitrogen. Crystals were precipitated and

settled directly in the settling chambers. A Sorvall continuous-flow centrifuge was used to concentrate algal and bacterial cultures.

Two systems were used for measuring absorbance. Aliquots of concentrated Scenedesmus, acid-cleaned N. pelliculosa frustules, and hypochlorite-treated Scenedesmus suspensions were dispensed to Plexiglas settling chambers (6.0 x 8.0 x 10.5 cm) and allowed to settle. Component density on the chamber base was adjusted by varying aliquot volume. After settling, excess medium was removed by aspiration to a standard depth. The chambers were made of transparent Plexiglas (0.64-cm thickness), which had nonselective absorbance and 89% transmittance of the incident radiance between 400 and 750 nm (Appendix C). This system was used for data presented in Figures 4, 5 upper, and 7.

A second system was employed for making light measurements which eliminated possible interference from light scattered by the Plexiglas chamber walls. This design also increased ease of sampling component density. Aliquots of components were pipetted from a well-mixed, concentrated suspension, dispensed to a volumetric cylinder, and brought to standard volume with the centrifugation supernatant. This suspension was then poured into a polystyrene petri dish (10.0 cm diameter x 1.5 cm depth) and allowed to settle with the dish on the diffuser plate of the spectroradiometer sensor. The polystyrene petri dishes had nonselective absorbance and transmitted 90% of the incident radiation between 400 and 750 nm (Appendix C). The petri dish system was used in absorbance measurements for the algae, bacteria, and calcium carbonate (Fig. 1, 2, 3, 5 lower, and 6).

A Techtum Instrument QSM-2500 spectroradiometer was used to measure

irradiance passing through the experimental components, media, and Plexiglas or polystyrene chambers. Chambers were placed directly on the diffuser plate of the sensor. Chamber bases were masked so that only light passing through the component was detected. An opaque, flatblack ring was placed over the top edge of the petri dish wall to prevent light scattered by the side walls from entering the sensor. The chamber base and sensor were positioned approximately 35 cm below a neutral diffuser and the light sources (two 15-watt General Electric Cool White and two 15-watt Luxor Vita Lite fluorescent tubes). The apparatus was enclosed in a light box. A Lambda voltage conditioner was used to stabilize the power supply to the fluorescent tubes. This light source simulated the light conditions of aquatic environments i.e., the light is diffuse with a strong directional component. The juxtaposition of the collector below the settled component approximates the spacial relationship of macrophyte chloroplasts and epiphyte layer. As a result, the light milieu at the collector surface closely approximates the light milieu at the macrophyte leaf surface. Distortion of absorbance values due to light scattered out of the path of the sensor was minimized by using a diffuse light source and settling the components over an area larger than the diffuse collector of the sensor. With this arrangement, the quantity of light incident upon the settled layer outside the collector area and scattered into the sensor was equivalent to the quantity of light incident upon the settled layer within the collector area and scattered away from the sensor.

Transmitted irradiance as quanta m^{-2} s^{-1} nm^{-1} was measured by scanning from 400 to 750 nm for each component and component density. Blanks were prepared by filtering media containing the component through

a Whatman GF/F glass fiber filter (95% retention of 0.7-μm particle diameter). Absorbances (A) were calculated at 10-nm intervals (i) from 400 to 750 nm for a particular component and density (j), by taking the $\log_{10}$ of the quotient for mean blank intensity for a particular 10-nm waveband and component (I_{ij}), divided by the mean intensity of irradiance passing through the particular component for that waveband and density (I'_{ij}), as:

$$A_{ij} = \log_{10} (I_{ij}/I'_{ij}). \qquad (1)$$

In order to make comparisons between components, component densities and mixtures of components, absorbance was normalized to mg dry weight (DW) resulting in extinction coefficients ($\varepsilon_{ij}=A_{ij}/DW_j$). The erratic nature of extinction coefficient spectra for the lowest densities of algae demarcated the lower limit of resolution for the apparatus.

Additional measures of absorbance by settled N. pelliculosa and the corresponding distributions of settled algal thicknesses were made. The distributions of settled algal thicknesses were also measured for Scenedesmus over the range of densities for which absorbances had previously been measured. Cells were settled in polystyrene petri dishes as described above. Transmission measurements were made for the Whatman GF/F glass fiber filtered medium blanks and samples at 440 nm with an Instrument Specialty Company (ISCO) spectroradiometer. The samples were settled for at least two hours before measurements were made with the petri dish positioned directly on the diffuser of the sensor. Six 15-watt Luxor Vita Lite fluorescent tubes were used as the light source. This source provided adequate intensity of 440 nm light to make transmission measurements with the spectroradiometer even at the greatest densities of settled algae.

Distribution of the thicknesses of settled cells was measured microscopically by randomly positioning the 40x water immersion objective of a Zeiss Standard RA microscope over the settled algae in the central portion of the petri dish. The thickness of settled algae was measured for the points in each microscope field located at the ends of the ocular micrometer graduations zero through nine. A total of 200 to 400 points were measured for each settled density by focusing on the upper most cell in the layer and noting the coarse/fine adjustment micrometer reading, and then refocusing on the lower most cell in the layer and noting the difference in micrometer readings to the nearest micrometer.

Densities of components on the Plexiglas base were determined by measuring dry weight of five 0.71 cm^2 area subsamples. After making transmission measurements, subsamples were aspirated from the base of the chambers through a tube pressed against the chamber base and sealed with a basal O-ring. The petri dish system was sampled with a much larger diameter tube (12.88 cm^2). Subsamples were filtered onto tared, precombusted (525°C), GF/F filters, and dried at 70°C for 48 hours, cooled, and weighed.

RESULTS

Absorbance values normalized for the density of settled material (mg dry weight per cm^2) yield an estimation of the specific extinction coefficient or absorbance per unit density per waveband of each periphyton component. Extinction coefficients of a waveband of radiation for different densities of a layered component are constant when absorbances for the different densities follow the Lambert-Beer relationship. The convention in this study has been to present extinction coefficient spectra in order to demonstrate the effect of density on periphyton component absorbances. With this method of presentation the PAR wavebands of maximum and minimum absorption and deviation of component absorbances from the Lambert-Beer relationship for all wavebands of the spectra can be evaluated. Periphyton component absorbances which follow the Lambert-Beer relationship would yield equivalent extinction coefficient spectra which overlie one another at different densities.

The relationship between absorbance spectra and normalized absorbance spectra, where there is no significant deviation from the Lambert-Beer relationship, was illustrated for five densities of Anabaena flos-aquae (Fig. 1 upper and lower, respectively). That absorbance by settled A. flos-aquae followed the Lambert-Beer relationship was illustrated by plotting absorbance versus density for the alga (Fig. 2). Peaks in the absorbance spectra of A. flos-aquae were found in the wavebands of 430-440 nm, 670-680 nm and 620-630 nm. These maxima correspond to the in vivo short and long wavelength absorption peaks of chlorophyll a and phycocyanins, respectively, the main pigments of blue-green (Cyanophyta) algae (Govindjee and Braun 1974).

Fig. 1. Absorbance spectra for five densities of settled Anabaena flos-aquae (upper). $A_{ij} = \log_{10} (I_i/I'_{ij})$ where I_i is mean intensity transmitted for the i^{th} 10-nm waveband, by a GF/F filtered algal medium blank, and I'_{ij} is the mean transmitted intensity for the i^{th} waveband and j^{th} density. Intensity measured as quanta m^{-2} s^{-1} nm^{-1}. Density was the oven-dried weight of the component settled on a 12.88 cm^2 area (mg DW cm^{-2}). Absorbance per unit density or extinction coefficient spectra (lower) for the five densities ($\varepsilon_{ij} = A_{ij}/mg\ DW_j\ cm^{-2}$).

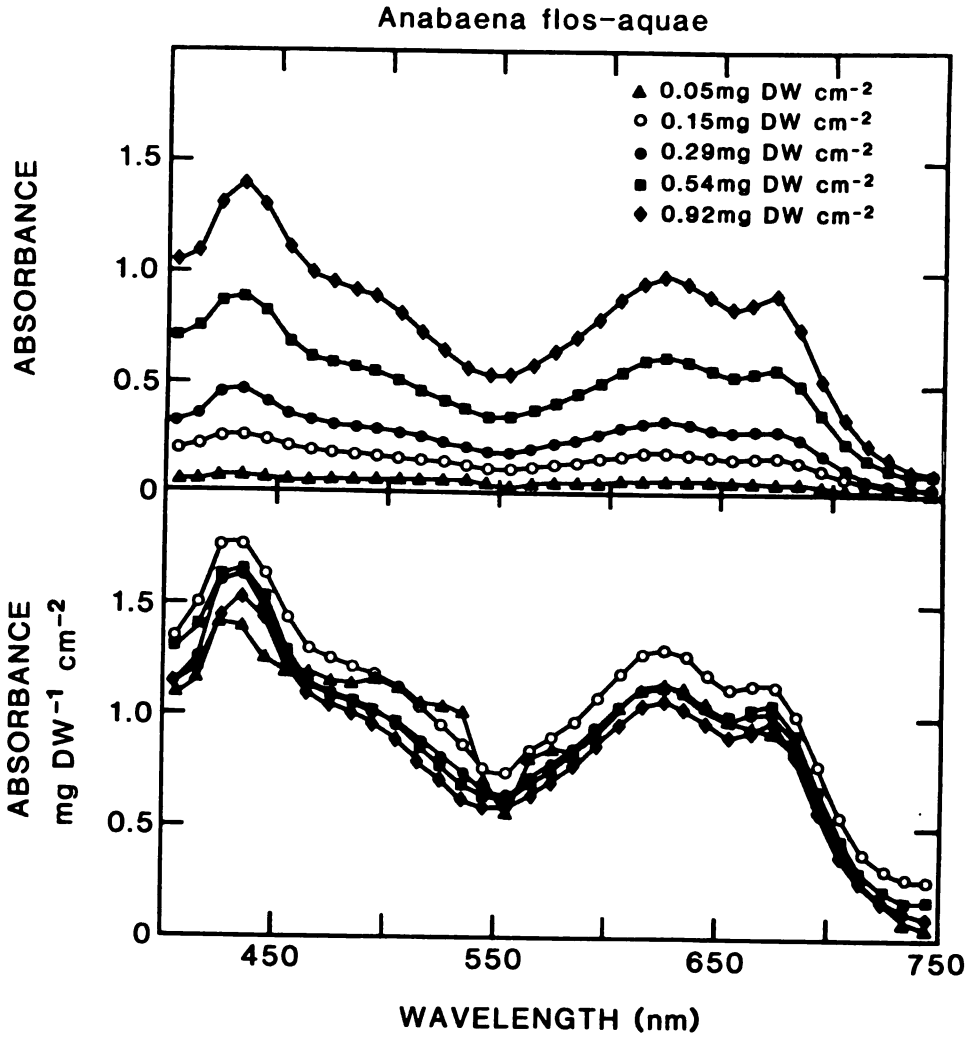
Anabaena flos-aquae
▲ 0.05mg DW cm-2
○ 0.15mg DW cm-2
● 0.29mg DW cm-2
■ 0.54mg DW cm-2
◆ 0.92mg DW cm-2
ABSORBANCE
1.5
1.0
0.5
0
ABSORBANCE
mg DW-1 cm-2
1.5
1.0
0.5
0
450
550
650
750
WAVELENGTH (nm)

Figure 1.

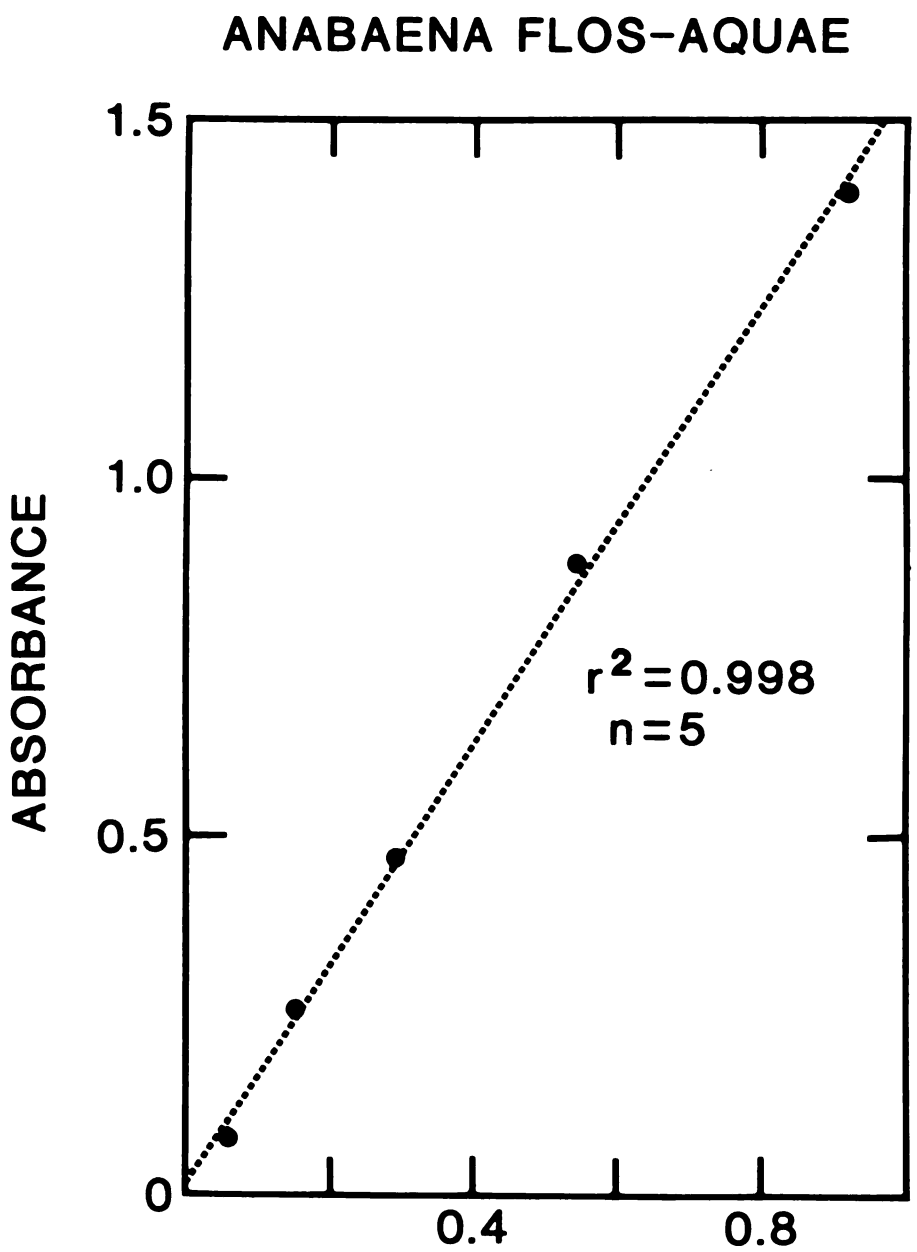

Fig. 2. Absorbance at 440 nm versus density for Anabaena flos-aquae. r^2 values are for least squares linear regression fit.

Absorbance maxima for the green alga (Chlorophyta) Scenedesmus (Fig. 3) were found to be in the wavebands corresponding to in vivo chlorophyll a (430-440 nm and 670-680 nm) and absorbance shoulders were found in the range for in vivo chlorophyll b (470-480 nm and 650-670 nm) (Govindjee and Braun, 1974). Absorbance by Scenedesmus cells bleached with hypochlorite to remove pigmentation had greatly reduced selectivity and attenuation in comparison to that of pigmented cells (Fig. 4). However, these cells with oxidized pigments maintained a small degree of selective absorbance at wavelengths less than 510 nm.

Broad absorbance peaks were found for the diatom (Chrysophyta) Navicula pelliculosa and for N. pelliculosa combined with Fragilaria crotonensis (Fig. 5 upper and lower, respectively), with maxima in the 420-440 nm and 670-680 nm wavebands. The absorbance shoulder in the range of 620 to 650 nm corresponded to in vivo chlorophyll c absorption (peak at 635 nm). The absorbance shoulder, which extended to greater than 550 nm on the chlorophyll a blue-waveband absorption peak, corresponded to in vivo β-carotene and fucoxanthin absorption regions (Govindjee and Braun, 1974). Acid-cleaned frustules of N. pelliculosa exhibited nonselective and very low absorbance (Fig. 5 upper).

Mixed bacteria also exhibited nonselective and low absorbance (Fig. 6). Absorbance by calcium carbonate crystals was nonselective and very low as well (Fig. 7).

Scenedesmus extinction coefficients were found to segregate into low and high density spectra. This segregation was illustrated in Figure 8 where absorbance at 440 nm has been plotted against settled algal density. The high density region was linear but the low density region had a consistent and less linear pattern.

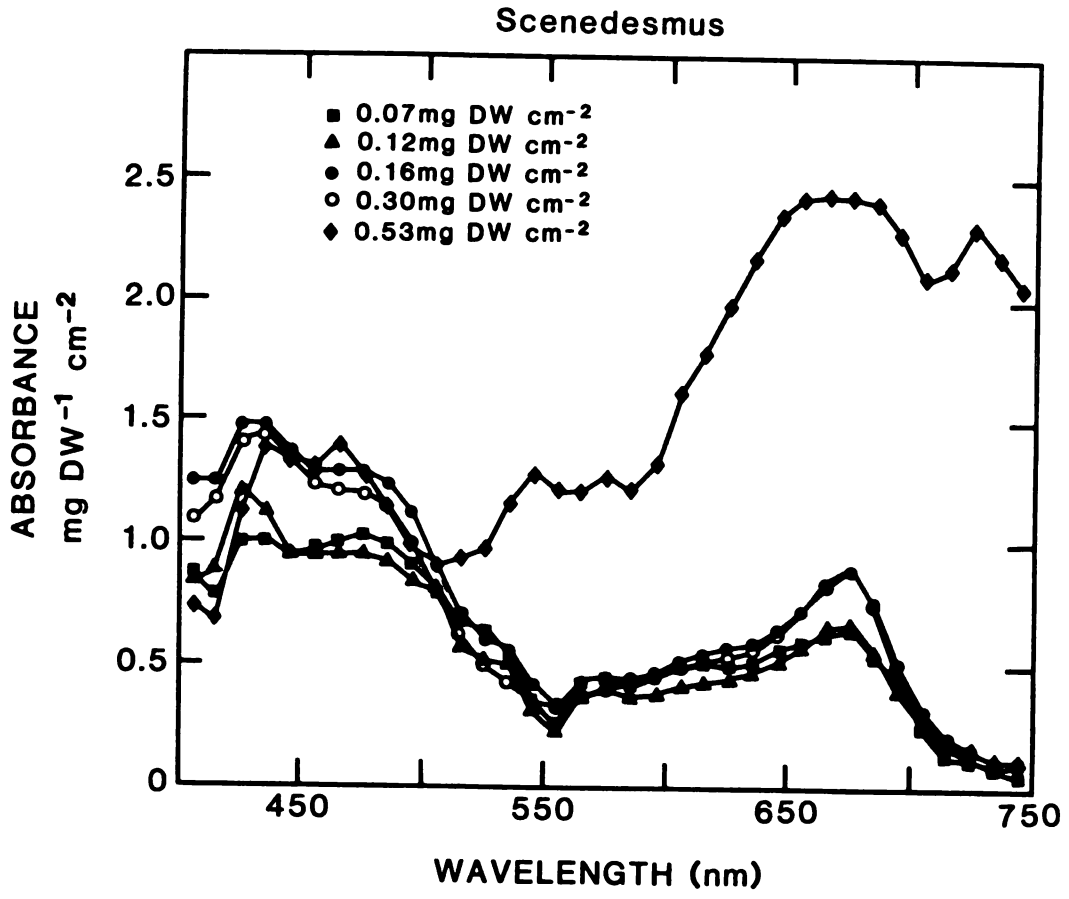

Fig. 3. Extinction coefficient (absorbance per unit density) spectra for five densities of settled Scenedesmus. See Fig. 1 for details.

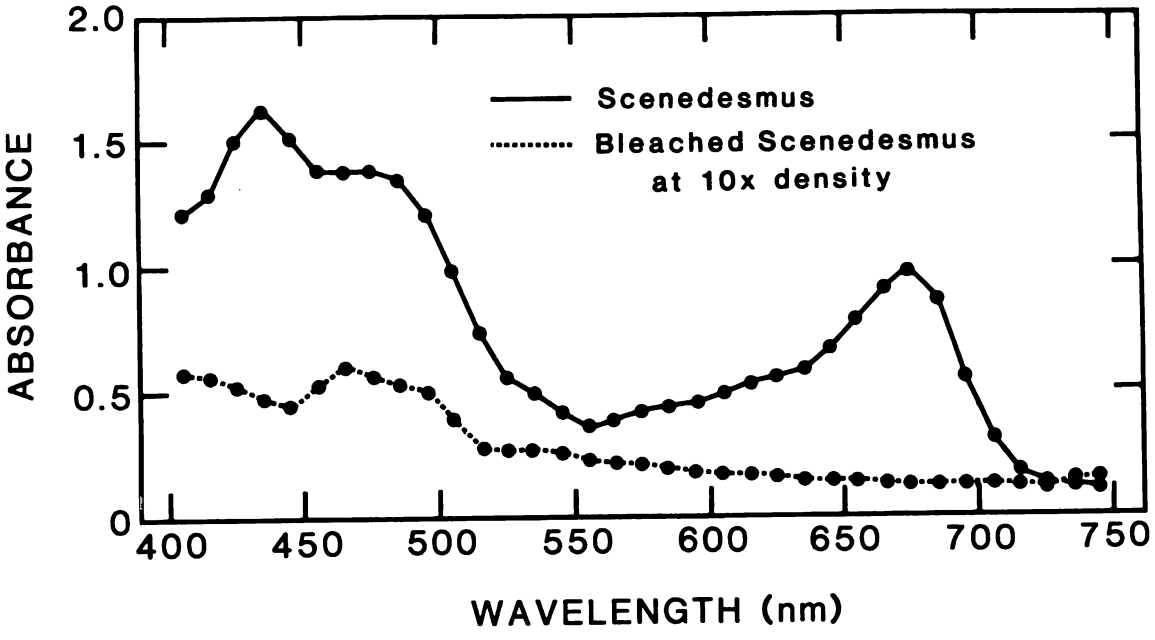

Fig. 4. Absorbance spectra for settled Scenedesmus (0.14 mg DW cm^{-2}) and hypochlorite-bleached Scenedesmus cells (1.5 mg DW cm^{-2}).

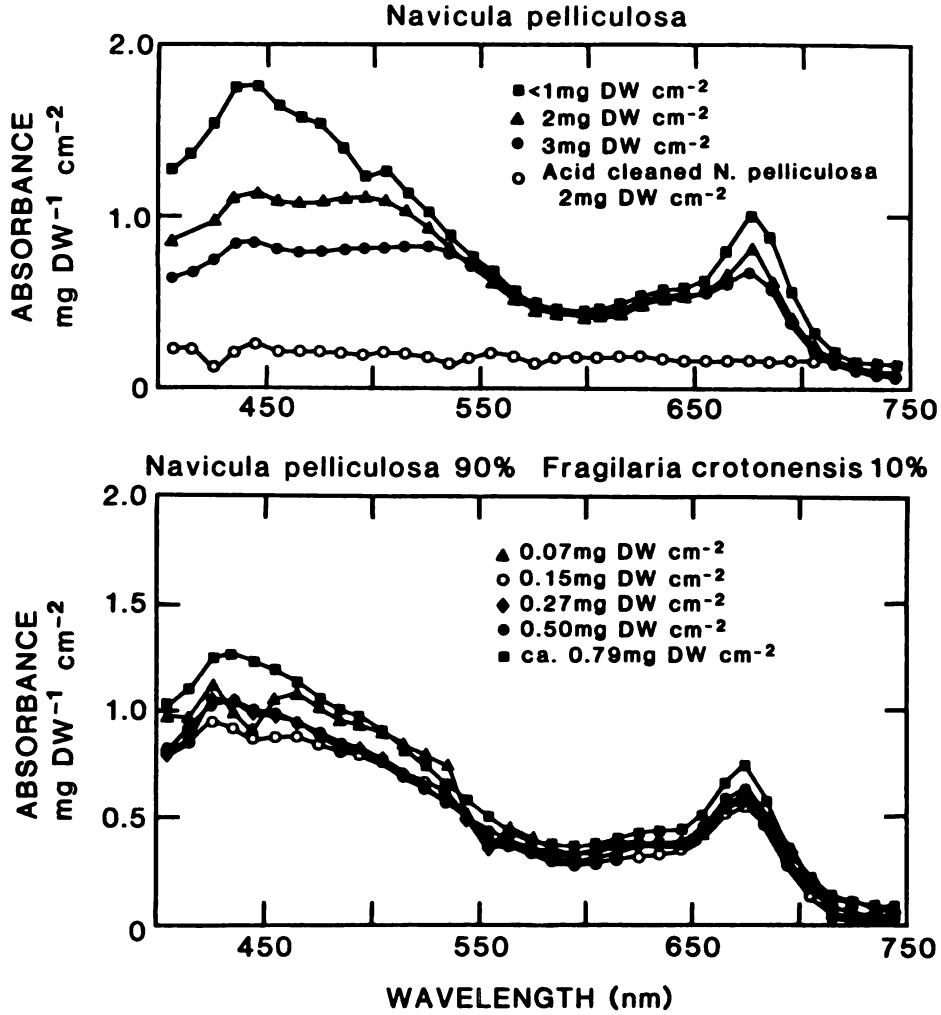

Fig. 5. Extinction coefficient spectra (absorbance per unit density) for four densities of the settled diatom Navicula pelliculosa and acid-cleaned N. pelliculosa frustules (upper), and for five densities of settled mixed diatoms (90% N. pelliculosa and 10% Fragilaria crotonensis by weight) (lower). See Fig. 1 for details.

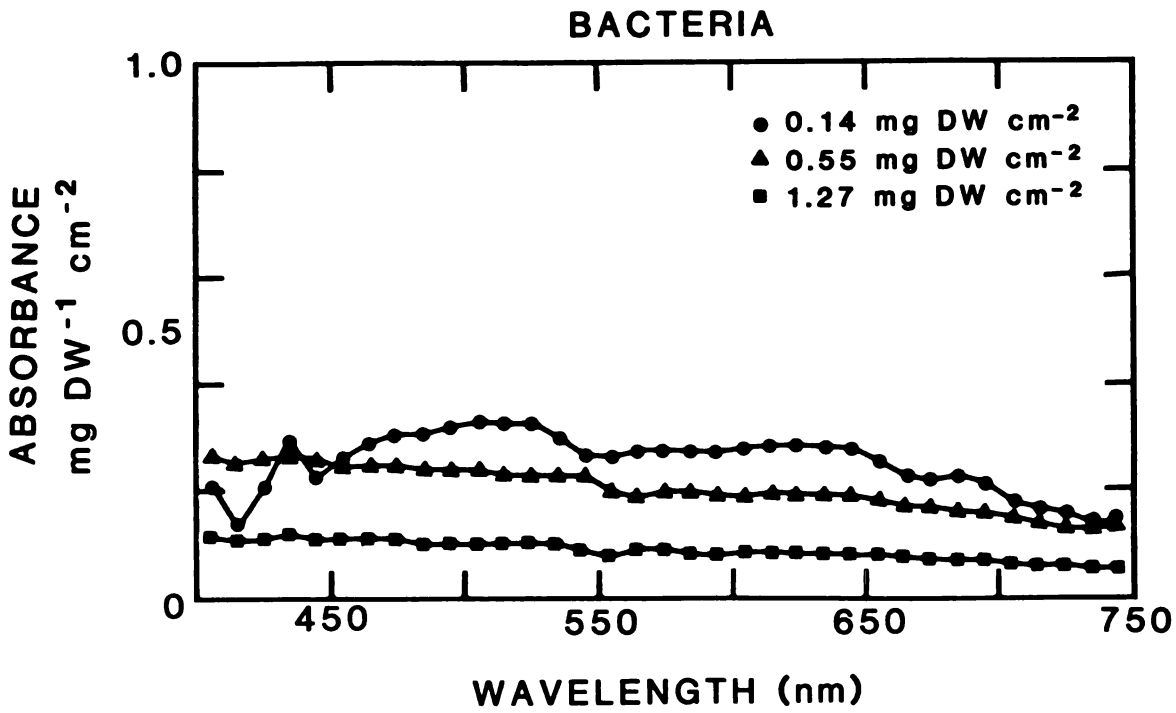

Fig. 6. Extinction coefficient spectra (absorbance per unit density) for three densities of settled bacteria. See Fig. 1 for details.

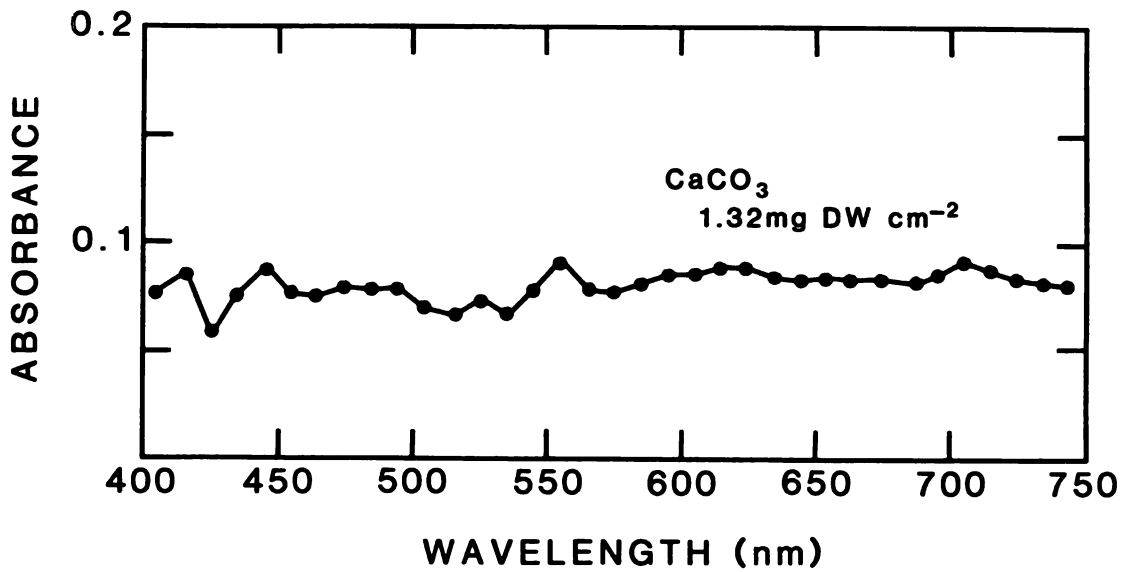

Fig. 7. Absorbance spectra for settled $CaCO_3$ (1.32 mg DW cm^{-2}).

The set of extinction coefficient spectra for N. pelliculosa (Fig. 5 upper) showed a trend of a decrease in absorbance per unit density as density was increased. This trend was apparent in a plot of absorbance at 440 nm versus density for two different cultures of N. pelliculosa. Figure 9a contains all absorbance data at 440 nm from samples used in Figure 5 upper. Data in Figure 9b were obtained from a N. pelliculosa culture inoculated from the same culture but at a later date. The distribution of settled algal thicknesses was measured concurrently with absorbance and density on these latter N. pelliculosa samples (Table 1, Appendix C). The distribution of settled Scenedesmus thicknesses for several densities was reported (Table 2, Appendix C), although absorbance measurements were not made for these samples.

DISCUSSION

The outstanding characteristic of periphyton component selective attenuation was absorption by algal photosynthetic pigments. Of these pigments, chlorophyll *a* was dominant. Algal accessory pigments, such as chlorophyll *b* and *c*, fucoxanthin, and phycocyanins, contributed to the absorption spectra by broadening the absorption bands around the red and blue chlorophyll *a* absorption peaks. Non-pigmented algal organic matter (e.g. hypochlorite-bleached *Scenedesmus* cells) was associated with relatively low absorption and much less selectivity. Bacteria, diatom frustules, and calcium carbonate crystals also exhibited low absorption and nonselectivity.

The intense absorption by epiphytic chlorophyll is particularly important because of the limited ability for chromatic adaptation in macrophytes. This is particularly true of submersed angiosperms which possess only chlorophyll *a* and *b* and photosynthetically inefficient carotenoids (Whittingham, 1976). Light intensity at the macrophyte leaf surface is generally maximal in the spectral range of 550 to 620-nm as a result of water column and epiphyton attenuation. This range is the spectral region of PAR which is least efficient in angiosperm photosynthesis. An increase in the chlorophyll content of macrophytes may ameliorate, to a degree, shading effects. Increased chlorophyll content has been reported in submersed macrophytes, particularly chlorophyll *b*, when plants were grown under reduced light conditions which resulted in a decrease in the chlorophyll *a*:*b* ratio (Van et al., 1977). Morphological adaptations have been noted in shaded leaves as well. Shade-adapted leaves of submersed macrophytes often show an

increased specific leaf area and diastrophic chloroplast positioning (reviewed by Spence, 1982).

Lambert-Beer's law states that successive increments in the number of identical absorbing molecules in the path of monochromatic radiation absorb equal fractions of radiant energy traversing them (i.e. $A=\varepsilon ci$ where A is absorbance, ε is the molar absorbance expressed in base 10 (or extinction coefficient), c is concentration and i is pathlength, and $T=10^{-\varepsilon ci}$, A=-log T where T is transmission). In periphyton, where spatial heterogeneity in the distribution of absorbing substances (i.e. photosynthetic pigments) occurs, different parts of the incident radiation intersect different quantities of pigment. This result is known as absorption statistics or the sieve effect. Transmission (and absorption) is the summation of elementary rays (or streams of photons) which traverse the periphyton layer. If only a single type of absorbing substance is present, then for any one ray the Lambert-Beer relationship is applicable, and the quantity of absorbing material intersected by the ray is a random magnitude with probability f(H,x), where H is layer thickness. In this investigation algal samples used for a particular set of light measurements came from the same culture and therefore, the pigment ratios of each algal cell were probably very similar. The specific distribution of photosynthetic pigments within algal cells was on a scale too small to measure. As a result, the reasonable assmumption that, on average, any algal area of unit thickness had equal extinction coefficient was implicit in light measurements.

Therefore, absorbance for the volume of periphyton above the area of the sensor (the sensor for a submersed macrophyte is the system of photosynthetic pigments) was:

$$A = \int_{\lambda=400}^{700} -\log \left[\int_{i=0}^{n} If(H,x)10^{-xd}dx/I \right] dy = \int_{\lambda=400}^{700} -\log \int_{i=0}^{n} f(H,x)10^{-dx}dxdy \qquad (1)$$

(Fukshansky, 1982). If f(H,x) is measured as the frequencies of discrete 1-μm thick classes for algae settled on the petri dish surface then, absorbance for a discrete distribution of layer thicknesses may be expressed as:

$$A_\lambda = -\log \Sigma(P_i)10^{-\varepsilon_\lambda ci} \qquad (2)$$

where (P_i) is the proportion of the petri dish surface covered by the i^{th} thickness class of settled algae, and λ is the wavelength of interest. If each μm thickness of an alga is assumed to have concentrations of absorbing substances with extiction coefficient ε_λ, then c may be assigned the value of one.

Absorbance at 440 nm versus density for Scenedesmus (Fig. 8) had a region of systematic deviation from linearity at low density and a linear region at higher density. Absorbance at 440 nm versus density for N. pelliculosa settled in Plexiglas chambers or polystyrene petri dishes (Figs. 9a and b, respectively) had two distinct regions: a low-density, steeply sloped region and a high-density region with a significantly lower sloped region (α=0.99).

The nonlinear region of the Scenedesmus absorbance versus density curve corresponded to the densities where, from equation (2), the proportion of the zero size class (P_0) (Table 1) was sufficiently greater than 0 to allow a greater quantity of light to be transmitted

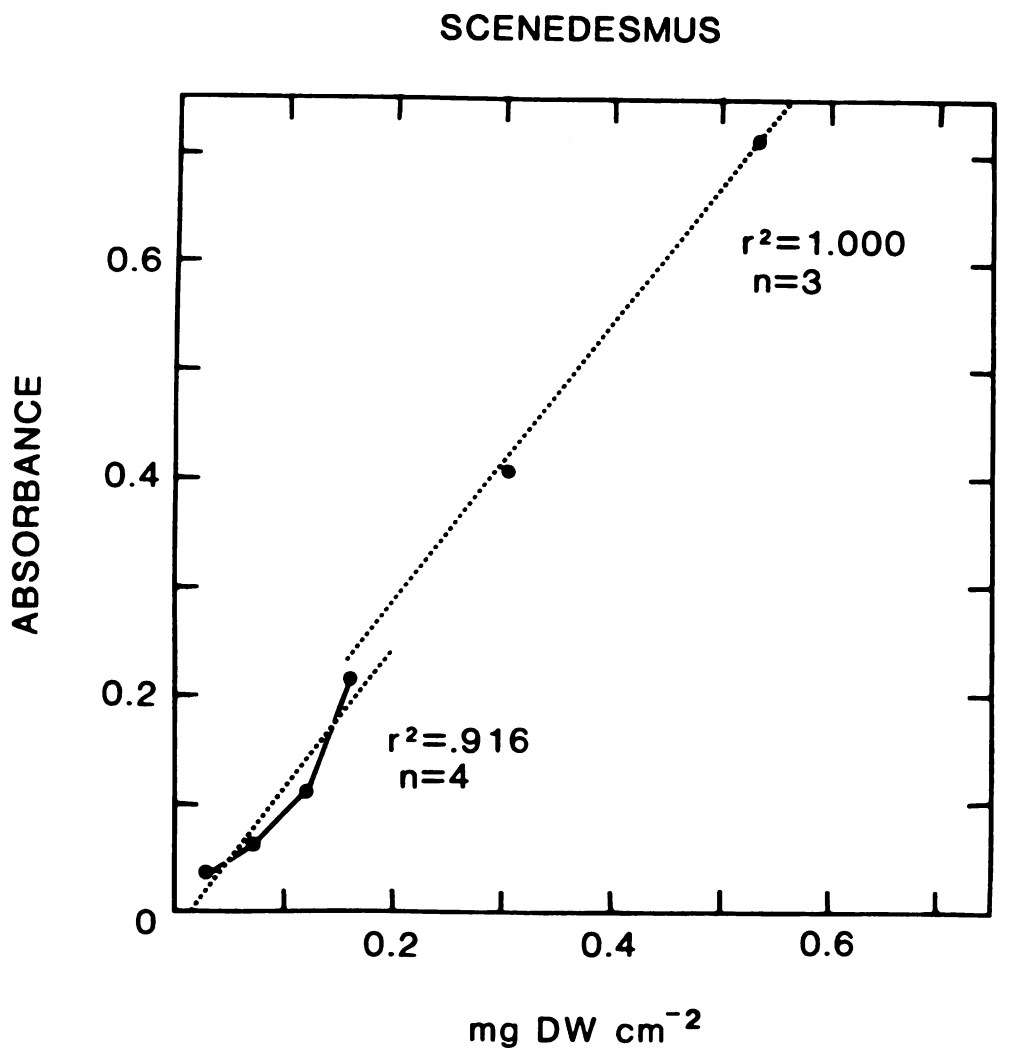

Fig. 8. Absorbance at 440 nm versus density for Scenedesmus. r^2 values are for least square linear regression fit for the seperate low density and high density regions. Note the systematic deviation from linearity of the low density region and linearity of the high density region.

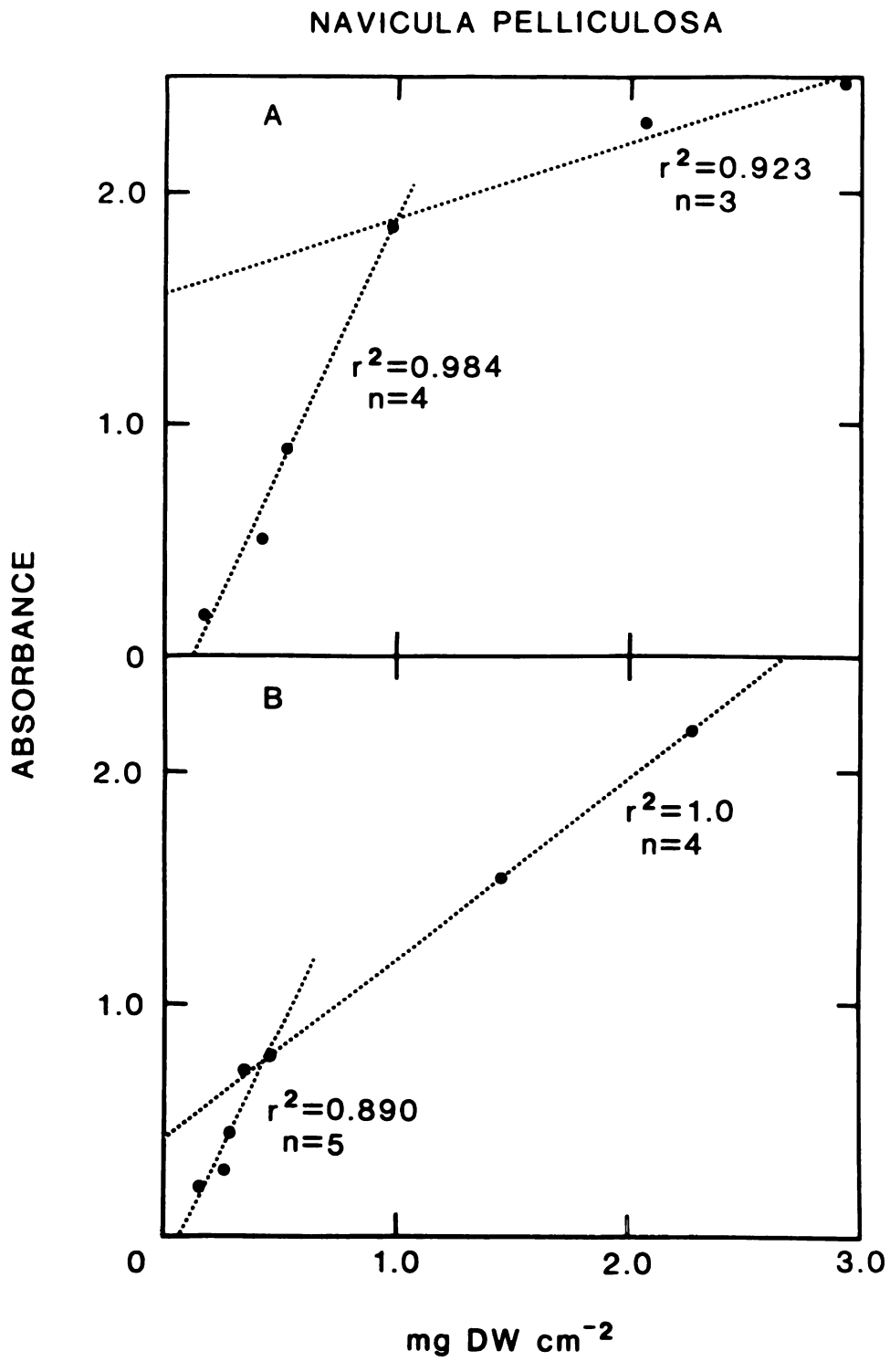

Fig. 9. Absorbance at 440 nm versus density for two cultures of N. pelliculosa. r^2 values are for least square linear regression fit for the high density and low density regions separately.

through the area free of cells than was transmitted through the area covered by cells. The transition point between the nonlinear and linear regions occurred at the density where P_0 was close to 0.

Table 1. Parameters characterizing the distribution of settled algal thicknesses (μm) for each density (mg DW cm^{-2}).

Density	Absorbance (440 nm)	Mode	Variance	Skewness/S.E.	P_0
Scenedesmus					
0.04	0.047	6.0	7.5040	6.56	0.480
0.07	0.068	7.0	15.4048	11.09	0.423
0.08	0.078	6.0	46.4589	21.48	0.254
0.10	0.104	5.0	7.7489	2.07	0.175
0.14	0.185	6.0	21.8236	6.10	0.135
0.15	0.208	5.0	13.7671	3.60	0.126
0.22	0.320	8.0	31.5653	20.94	0.030
0.32	0.465	13.0	34.3638	5.40	0.000
N. pelliculosa					
0.148	0.211	4.0	4.7260	1.67	0.135
0.256	0.283	4.0	5.9196	3.47	0.070
0.288	0.451	5.0	23.2850	6.32	0.050
0.358	0.715	5.0	6.9536	3.29	0.015
0.442	0.755	10.0	11.3108	4.55	0.000
1.462	1.561	21.0	30.2589	5.98	0.000
2.271	2.184	26.0	11.4812	4.78	0.000

The distributions of settled algal thicknesses were measured concurrently with absorbance for the *N. pelliculosa* samples of Figure 9b (Table 1). The transition point between the low-density, steeply sloped and high-density, less steeply sloped regions for the settled alga corresponded to the point where $P_0=0$ (Fig. 9b). The differences in the absorbances for the two cultures of *N. pelliculosa* were most likely the result of two factors: First, a difference in the distribution of settled algal thicknesses could have been caused by different microscale current patterns in the Plexiglas (Fig. 9a) and petri dish chambers

(Fig. 9b) where media depths were different (>2.0 cm, 0.5 cm media depth, respectively). Secondly, although the inocula for both cultures were taken from the same line of stock culture, the algae of Figure 9b were cultured several months later and cells of this latter culture were larger.

Absorbance was regressed on the parameters of table 1, which characterize the distribution of settled algal thicknesses (mode, p_0, variance, skewness/standard error), using appropriate least squares stepwise regression (BMDP, 1982). For the lower density regions of both algae, it was found that P_0 was the only parameter which contributed significantly to the fit of the model (adjusted r^2= 0.69 and 0.83 for Scenedesmus and N. pelliculosa, respectively). For the high density region the mode of the distribution of layer thicknesses was the only parameter which could be shown to significantly contribute to the fit of the model (adjusted r^2= 0.74 and 0.91 for Scendesmus and N. pelliculosa, respectively).

A regression of density on absorbance for Anabaena flos-aquae showed no significant deviation from linearity (adjusted r^2=0.998) and plotting absorbances did not suggest the existence of any small, systematic deviation from linearity (Fig. 2). A relatively uniform cellular pigment distribution and sheet-forming filamentous growth form were observed microscopically at low densities of settled A. flos-aquae. The constant extinction coefficient found for A. flos-aquae as density was changed probably resulted from a relatively uniform layer thickness at all algal densities. The sheet-like colonies of this alga were one cell thick, and as a result, could only settle on the broad side of the colonies. Consequently, there was small probability that cells would pile with

more than a few cells deviation from uniform thickness at any point.

These data illustrate the importance of physical structure of the epiphyton layer in light attenuation. Light attenuation in the epiphytic layer will be greatly reduced by the exclusion of photosynthetic pigment from portions of the layer. Clustering or clumping of algae, as might occur when colonial algae colonize a macrophyte surface, would yield a reduction in attenuation. Dead diatoms, in which pigments have been bleached by a combination of microbial action and photooxidation (Daley, 1973), would act as an excellent conduit for the transmission of light through the layer of algal photosynthetic pigments.

For example, absorbance values for the mixed diatoms were lower than for equal densities of N. pelliculosa alone. F. crotonensis cells were approximately four times the length of the N. pelliculosa cells and formed ribbon-like colonies with cells attached valve to valve. Additionally, N. pelliculosa were much more densely pigmented than were F. crotonensis. Microscopic examination revealed that, when settled, the F. crotonensis cells traversed the layer of N. pelliculosa cells and thereby provided a pathway of lower absorption through the layer. Calcium carbonate crystals may also act to conduct light through the periphyton layer. The effectiveness of these crystals as light conductors increases with increasing crystal size. A high density of very small crystals (linear dimensions less than those of periphytic algae) would probably increase attenuation as a result of reflection off the crystal surfaces and the concomitant increase in light ray pathlength and consequential pigment intersection. Carbonate crystals found on a Potamogeton illinoensis Morong. leaf, ranged in linear dimensions from very small (3 μm) to large (>15 μm). Qualitative observation showed

that the distribution of crystal sizes was strongly skewed toward the larger sizes. Carbonate crystals in this size range were also found, precipitated out of the water column, in the seston at six meters in calcarious Lawrence Lake (White, 1974). Crystals of sufficient size to reduce epiphytic light attenuation apparently are common in calcarious systems. However, absorption of PAR by humic substances embedded within or adsorbed to carbonate crystals may be significant in humic rich waters and should be quantified in any further study of periphyton light attenuation.

Apparent absorbance of PAR by nonselective and low light absorbing bacteria and calcium carbonate crystals was almost entirely the result of scattering. Particles in the size ranges of bacteria and carbonate crystals scatter light at low angles (Koch, 1970). Despite its diffusivity, the light source used in the absorption measuring apparatus provided strongly directionally oriented light. Part of the light scattered by a particle in the settled layer would be secondarily scattered by another particle and reoriented so that it fell upon the detector (Koch, 1970). The frequency of this occurrence, of course, would increase as layer thickness was increased. This effect resulted in the decrease in extinction coefficient with increasing density as observed for bacteria and calcium carbonate. Further support for the importance of scattering in bacterial and carbonate components apparent absorbances was that the magnitude of the differences in extinction coefficients decreased at longer wavelengths as density was changed, (Koch, 1970; Kavanagh, 1972).

The marked increase in absorbance and broadening of the long-wavelength peak at the greatest density of Scenedesmus (0.53 mg cm^{-2})

(Fig. 8) is not fully understood at this time. However, the shift in the absorbance spectrum may be the result of chlorophyll fluorescence at the shorter wavelengths. If this observation and speculation is correct, then macrophytes and other algal epiphytes in association with this Scenedesmus might be benefited by a shift in their action spectra to shorter wavelengths.

Measurement of periphyton community shading effects on submersed macrophytes in the field is complicated by many factors. Periphyton may reduce plant growth and photosynthetic rates by competing for nutrients, acting as a barrier to inorganic carbon, and by reducing available PAR. When measuring productivity, it is extremely difficult to separate productivity of the tightly attached epiphytes from that of the macrophyte. Where estimates of macrophyte and epiphyte productivity have been made separately, epiphyte densities were not measured in a manner comparable to that used in this study. There are many other potentially confounding factors concerning macrophyte productivity measurements in relation to epiphyte densities. For example, the epiphytic community is dynamic, continuously changing density and composition as the macrophyte-periphyton complex ages and the substrata changes size and physiological condition.

As an example of the effects of light attenuation on macrophytes, the PAR at the leaf surface of the submersed macrophyte Myriophyllum spicatum L., at some depth in the water column and for various periphyton components and component densities was calculated and these light levels were used to predict photosynthetic rates under the various epiphyte loads. These photosynthetic rates were based on experimentally determined photosynthetic rates for the resultant PAR levels (Van et

al., 1976).

In order to estimate the potential shading effects of periphyton components, it was necessary to make several simplifying assumptions. It was assumed that M. spicatum photosynthetic rates were unaffected by the spectral distribution of PAR because Van et al. (1976) based their photosynthetic rate determinations on an integrated measure of PAR. This was an important assumption because of the spectral shift caused by the algal periphyton which would result in the inclusion of a greater proportion of green light. Further, as stated above, the caroteniod pigments of angiosperms, which absorbs light in the green region of the spectrum, are only half as efficient as chlorophyll in producing photosynthesis. However, the use of PAR here was adequate to provide an indication of component shading effects. It was also assumed that a single component was uniformly distributed on the leaf surface resulting in maximum reduction in PAR for the component density. Finally, it was assumed that the only periphyton component effect on photosynthetic rate was a result of light attenuation. As noted earlier, periphyton may act as a barrier to inorganic carbon diffusion. However, in the one known study which has investigated light attenuation and inorganic carbon barrier effects of periphyton, it was concluded that at the natural bicarbonate concentration (1.7 meq l^{-1}), the barrier effect would decrease photosynthetic rates appreciably only at very high light levels (Sand-Jensen, 1977).

The derived photosynthetic rates for components at several densities indicated that, among periphytic algal components, mixed diatoms least affected photosynthetic rates of M. Spicatum (Table 2). For these calculations, density was measured as component dry weight per cm^{-2}.

Therefore, the dense, silicious frustule of the diatoms resulted in a lower algal volume per unit density for diatoms compared to the green and blue-green algae. However, the diatom frustule is highly transparent and, therefore, on a volume basis, would also attenuate less light than green and blue-green algae. Calcium carbonate was calculated to exert a relatively minor shading effect compared to algae. Even at the maximum carbonate density reported by Kowalczewski (1975) of 2.8 mg DW cm^{-2} and the conditions and assumptions of Table 2, the reduction in M. spicatum photosynthetic rate resulting from carbonate shading would only be 7.5 percent.

Table 2. Percent reduction in photosynthetic rates (μmole CO_2 mg Chl^{-1} h^{-1}) derived from the experimentally determined photosynthetic light curve for Myriophyllum spicatum (Van et al., 1976) and component absorbances calculated for each component density. $I'=I\ 10^{-A}$, where I' is PAR intensity at the leaf surface, I is the ambient PAR intensity, and $A=\varepsilon D$, where ε is the approximate mean component extinction coefficient for all wavebands, and D is the component density.

		Density (mg DW cm^{-2})			
Component	(ε)	0	0.25	0.5	1.0
Diatoms (mixed)	0.45	0%	5%	10%	31%
Green algae	0.75	0%	8%	23%	56%
Blue-green algae	1.0	0%	11%	34%	97%
Bacteria	0.15	0%	3%	3%	7%
$CaCO_3$	0.06	0%	2%	3%	3%

Examples of mechanisms which allow submersed aquatic macrophytes to survive where planktonic and epiphytic microflora are abundant are known. Submersed plants often have low-light compensation points as in Hydrilla verticillata (L.F.) Royle and M. spicatum, 15 and 35 $\mu E\ m^{-2}s^{-1}$, respectively. Submersed Juncus bulbosus L. possesses an even lower light compensation point of 1.5 $\mu E\ m^{-2}s^{-1}$ (Wetzel et al., 1983). H. verticillata utilize the large energy store of their overwintering structures for rapid growth early in the growing season and form a dense canopy at the water surface (Van et al., 1977). High in the water column just below the surface there is sufficient light for these plants to survive even with a relatively dense epiphyte load. M. spicatum is capable of very rapid shoot elongation exceeding 1 cm per day (Wetzel, personal commun.). Other strategies in aquatic plants may also indicate the importance of light to the survival of epiphytized macrophytes. For example, eelgrass (Zostera marina L.) exhibits rapid turnover of leaves. Sand-Jensen (1977) has hypothezised that this rapid replacement of photosynthetic tissue is a response to epiphytic colonization, with the macrophyte essentially out growing epiphyte colonization.

Aquatic habitats are light-limited environments. Epiphytic algal photosynthetic pigments contribute to light attenuation by absorbing very strongly in the wavelengths which submersed macrophytes may efficiently utilize for photosynthesis. It is concluded that the severity of light attenuation is a function of the community components present, component geometry, and the distribution of components within the epiphyton.

APPENDICIES

APPENDIX A

MBG Medium

	MW	Final Conc. Molar	Final Conc. mg l^{-1}	500x Stock g l^{-1}	ml Stock l^{-1} Medium
1. $NaNO_3$	85	3.0mM	255.0	127.5	2 ml
2. KH_2PO_4	136	0.23	31.3	15.6	2 ml
3. $MgSO_4$ $7H_2O$	246	0.25	61.5	30.8	2 ml
4. $CaCl_2$ or	111	0.30	41.1	16.7	2 ml
$CaCl_2$ $2H_2O$	147	0.30	41.1	22.1	2 ml
5. $KHCO_3$	100	1.0	100.0	50.0	2 ml
6. Fe-Na-EDTA	367	20.0 µM	7.34	1.84	4 ml
7. Na_2EDTA $2H_2O$	372	10.0	3.9	1.94	2 ml
8. $MnCl_2$ H_2O	198	5.0	0.99	0.495	2 ml
$ZnCl_2$	136	0.5	0.068	0.034	2 ml
$NaMoO_4$ $2H_2O$	242	1.5	0.363	0.182	2 ml
$CuCl_2$	135	0.04	0.0054	0.0027	2 ml
$CoCl_2$ $6H_2O$	238	0.15	0.0357	0.0179	2 ml
H_3BO_3	61.8	40.0	2.47	1.24	2 ml
9. Na_2SiO_3 $9H_2O$	284	0.5mM	142.0	14.2	10 ml *
10. Tricine	179.2	2.0	358.0	35.8 (100x)	10 ml **

11. Vitamins

Thiamine HCl 0.1 mg l^{-1}

Biotin 0.5 µg l^{-1}

Cyanocobalamin (B_{12}) 0.5 µg l^{-1}

Autoclave vitamins separately from medium.

* Preparation of stock (to prevent polymerization)

  - Weigh 14.2 g $NaSiO_3$ $9H_2O$ into beaker.

  - Add 0.5 ml conc. H_2SO_4 and adjust to pH 8.0 with dilute acid.

  - Transfer to 1 liter volumetric flask and dilute to volume.

** Preparation of Tricine stock (pH 8.0), (100 ml)

  - Weigh 3.58 g Tricine (desic.) into 100 ml volumetric flask.

  - Add 6.4 ml 1N NaOH.

  - Bring to volume with double distilled water.

APPENDIX B

Epiphytic Scenedesmus Isolation

Algal cells were scraped from aquarium-grown Najas flexilis leaves, diluted in MBG medium (Appendix A), and shaken to disperse cells. Five culture flasks containing 100 ml of MBG medium were inoculated with 0.2 ml of diluted cell suspension. After a two week incubation, it became apparent by microscopic observation that two flasks were dominated by green algae, two by blue-green algae and one by diatoms.

A wire loop was used to scrape algal cells from the flask walls of the green algae dominated culture. Cells were streak-plated onto Difco Bacto 'algae culture agar' and incubated for two weeks. Several algal colonies developed. Colonies were used to inoculate individual 100-ml MBG media culture flasks. After two additional weeks of incubation, cultures were checked for monospecificity. From the culture with the fewest species, aliquots of the algal suspension were concentrated by centrifugation. In an effort to mechanically free the algal cells of bacterial contamination, the pellet of algal cells was resuspended in sterile medium and centrifuged three times. After the final rinse the algal cells were suspended in 25 ml of medium. One ml of suspension was diluted three times serially with 25 ml of medium which resulted in an approximate 25^3 times final dilution.

An antibiotic solution was prepared by mixing 100 mg penicillin G and 50 mg streptomycin SO_4 in 10 ml distilled water and adding 10 mg chloramphenical dissolved in 1 ml 95% ethanol. The solution was quickly filtered using a 0.2-μm pore size Nuclepore membrane. The antibiotic solution was added to 25 ml of MBG medium in 50-ml culture tubes in the

following volumes: 1.5, 1.0 and 0.125 ml.

0.2 ml of the diluted cell suspension was added in triplicate to test tubes at each antibiotic level. After two days, aliquots from each antibiotic-media culture were transferred to antibiotic-free media. After algal growth was evident in test tubes these cultures were examined microscopically for monospecificity. No sterility test was performed on the culture.

APPENDIX C

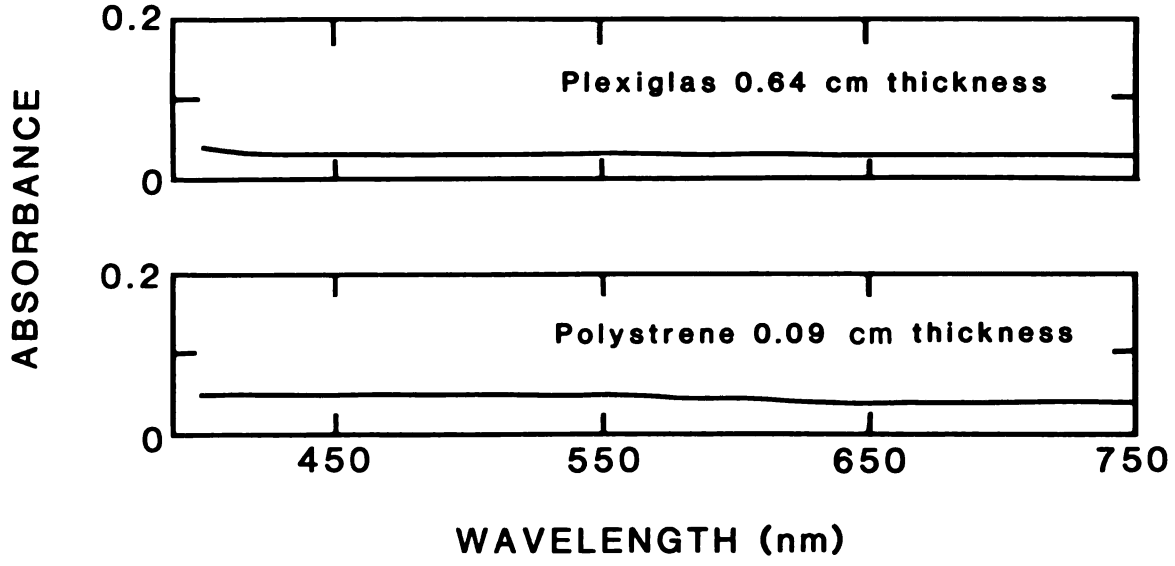

Absorbance spectra of Plexiglas (0.64-cm thickness), upper, and Polystyrene (0.09-cm thickness), lower. Absorbance measurements were made with a Beckman DU-8 spectrophotometer.

APPENDIX D

Table 1. Proportional distribution of settled *Navicula pelliculosa* thicknesses.

Size class	Proportion of surface covered by μm size class thicknesses for settled algae in density (mg DW cm^{-2}) categories.						
(μm)	0.148	0.256	0.288	0.358	0.442	1.462	2.271
0	0.135	0.070	0.050	0.450	0.000	0.000	0.000
1	0.090	0.090	0.058	0.015	0.000	0.000	0.000
2	0.135	0.120	0.043	0.050	0.000	0.000	0.000
3	0.075	0.115	0.083	0.070	0.000	0.000	0.000
4	0.155	0.155	0.078	0.085	0.010	0.000	0.000
5	0.145	0.150	0.123	0.100	0.025	0.000	0.000
6	0.140	0.120	0.930	0.180	0.040	0.000	0.000
7	0.065	0.060	0.078	0.155	0.075	0.000	0.000
8	0.025	0.055	0.073	0.120	0.100	0.000	0.000
9	0.025	0.035	0.038	0.080	0.100	0.000	0.000
10	0.005	0.020	0.060	0.030	0.175	0.000	0.000
11	0.005	0.005	0.045	0.040	0.135	0.000	0.000
12	0.000	0.000	0.025	0.020	0.070	0.000	0.000
13	0.000	0.000	0.020	0.005	0.090	0.003	0.000
14	0.000	0.005	0.018	0.015	0.075	0.007	0.000
15	0.000	0.000	0.030	0.000	0.025	0.010	0.000
16	0.000	0.000	0.015	0.005	0.040	0.023	0.000
17	0.000	0.000	0.010	0.000	0.015	0.036	0.000
18	0.000	0.000	0.013	0.000	0.005	0.030	0.000
19	0.000	0.000	0.010	0.000	0.005	0.062	0.000
20	0.000	0.000	0.008	0.000	0.005	0.075	0.008
21	0.000	0.000	0.013	0.000	0.010	0.072	0.004
22	0.000	0.000	0.000	0.000	0.005	0.102	0.036
23	0.000	0.000	0.000	0.000	0.005	0.085	0.020
24	0.000	0.000	0.005	0.000	0.000	0.062	0.087
25	0.000	0.000	0.008	0.000	0.000	0.049	0.131
26	0.000	0.000	0.000	0.000	0.000	0.056	0.135
27	0.000	0.000	0.003	0.000	0.000	0.059	0.095
28	0.000	0.000	0.000	0.000	0.000	0.033	0.107
29	0.000	0.000	0.000	0.000	0.000	0.030	0.111
30	0.000	0.000	0.000	0.000	0.000	0.020	0.067
31	0.000	0.000	0.003	0.000	0.000	0.026	0.079
32	0.000	0.000	0.003	0.000	0.000	0.030	0.044
33	0.000	0.000	0.000	0.000	0.000	0.016	0.020
34	0.000	0.000	0.000	0.000	0.000	0.013	0.032
35	0.000	0.000	0.000	0.000	0.000	0.007	0.008
36	0.000	0.000	0.000	0.000	0.000	0.003	0.004
37	0.000	0.000	0.000	0.000	0.000	0.023	0.012
38	0.000	0.000	0.000	0.000	0.000	0.003	0.004
39	0.000	0.000	0.000	0.000	0.000	0.007	0.004
40	0.000	0.000	0.000	0.000	0.000	0.003	0.000

Table 1 (cont'd.).

Size class	Proportion of surface covered by μm size class thickness of settled algae in density (mg DW cm^{-2}) categories.						
(μm)	0.148	0.256	0.288	0.358	0.442	1.462	2.271
41	0.000	0.000	0.000	0.000	0.000	0.000	0.012
42	0.000	0.000	0.000	0.000	0.000	0.003	0.004
43	0.000	0.000	0.000	0.000	0.000	0.007	0.000
44	0.000	0.000	0.000	0.000	0.000	0.013	0.000
45	0.000	0.000	0.000	0.000	0.000	0.000	0.004
46	0.000	0.000	0.000	0.000	0.000	0.000	0.000
47	0.000	0.000	0.000	0.000	0.000	0.003	0.000
48	0.000	0.000	0.000	0.000	0.000	0.000	0.000
49	0.000	0.000	0.000	0.000	0.000	0.003	0.000
50	0.000	0.000	0.000	0.000	0.000	0.000	0.000
51	0.000	0.000	0.000	0.000	0.000	0.000	0.000
52	0.000	0.000	0.000	0.000	0.000	0.003	0.000

Table 2. Proportional distribution of settled Scenedesmus thicknesses.

Size class	Proportion of surface covered by μm size class thickness for settled algal density (mg DW cm^{-2}) categories.							
(μm)	0.04	0.07	0.08	0.10	0.14	0.15	0.22	0.32
0	0.480	0.425	0.255	0.175	0.135	0.120	0.030	0.000
1	0.000	0.005	0.005	0.015	0.015	0.025	0.005	0.000
2	0.005	0.005	0.035	0.050	0.025	0.025	0.020	0.000
3	0.015	0.025	0.020	0.040	0.055	0.065	0.020	0.000
4	0.050	0.070	0.055	0.070	0.075	0.095	0.030	0.015
5	0.085	0.050	0.075	0.140	0.090	0.161	0.075	0.020
6	0.110	0.075	0.105	0.120	0.120	0.085	0.050	0.030
7	0.075	0.090	0.085	0.115	0.090	0.025	0.104	0.085
8	0.075	0.070	0.095	0.065	0.065	0.106	0.085	0.060
9	0.040	0.070	0.025	0.095	0.070	0.075	0.065	0.050
10	0.025	0.035	0.070	0.060	0.055	0.040	0.104	0.050
11	0.015	0.035	0.060	0.020	0.040	0.050	0.080	0.317
12	0.005	0.015	0.030	0.005	0.035	0.025	0.085	0.070
13	0.000	0.000	0.015	0.015	0.015	0.035	0.065	0.106
14	0.005	0.015	0.005	0.010	0.015	0.020	0.045	0.080
15	0.005	0.005	0.020	0.005	0.035	0.015	0.040	0.060
16	0.000	0.005	0.005	0.000	0.000	0.010	0.025	0.060
17	0.000	0.000	0.015	0.000	0.015	0.010	0.020	0.060
18	0.010	0.000	0.005	0.000	0.000	0.005	0.015	0.055
19	0.000	0.000	0.005	0.000	0.010	0.000	0.010	0.040
20	0.000	0.000	0.005	0.000	0.020	0.000	0.015	0.020
21	0.000	0.000	0.000	0.000	0.005	0.000	0.005	0.040
22	0.000	0.000	0.000	0.000	0.005	0.000	0.000	0.010
23	0.000	0.000	0.000	0.000	0.010	0.000	0.000	0.010
24	0.000	0.000	0.000	0.000	0.000	0.000	0.000	0.010
25	0.000	0.000	0.000	0.000	0.000	0.000	0.000	0.010
26	0.000	0.005	0.000	0.000	0.000	0.000	0.000	0.005
27	0.000	0.000	0.000	0.000	0.000	0.000	0.000	0.005
28	0.000	0.000	0.000	0.000	0.000	0.000	0.000	0.010
29	0.000	0.000	0.000	0.000	0.000	0.000	0.000	0.000
30	0.000	0.005	0.000	0.000	0.000	0.000	0.000	0.005
31	0.000	0.000	0.000	0.000	0.000	0.000	0.000	0.005
32	0.000	0.000	0.000	0.000	0.000	0.000	0.005	0.005
33	0.000	0.000	0.000	0.000	0.000	0.000	0.000	0.005
34	0.000	0.000	0.000	0.000	0.000	0.000	0.000	0.005
35	0.000	0.000	0.000	0.000	0.000	0.000	0.000	0.005
36	0.000	0.000	0.005	0.000	0.000	0.000	0.000	0.000
37	0.000	0.000	0.000	0.000	0.000	0.000	0.000	0.000
38	0.000	0.000	0.000	0.000	0.000	0.000	0.000	0.000
39	0.000	0.000	0.000	0.000	0.000	0.000	0.000	0.000
40	0.000	0.000	0.000	0.000	0.000	0.000	0.000	0.000
41	0.000	0.000	0.000	0.000	0.000	0.000	0.000	0.000
42	0.000	0.000	0.000	0.000	0.000	0.000	0.000	0.000
43	0.000	0.000	0.000	0.000	0.000	0.000	0.000	0.000
44	0.000	0.000	0.000	0.000	0.000	0.000	0.000	0.000
45	0.000	0.000	0.000	0.000	0.000	0.000	0.000	0.000

Table 2. (cont'd.).

Size class	Proportion of surface covered by μm size class thickness for settled algal density (mg DW cm^{-2}) categories.							
(μm)	0.04	0.07	0.08	0.10	0.14	0.15	0.22	0.32
46	0.000	0.000	0.000	0.000	0.000	0.000	0.000	0.000
47	0.000	0.000	0.000	0.000	0.000	0.000	0.000	0.000
48	0.000	0.000	0.000	0.000	0.000	0.000	0.000	0.000
49	0.000	0.000	0.000	0.000	0.000	0.000	0.000	0.000
50	0.000	0.000	0.005	0.000	0.000	0.000	0.000	0.000
51	0.000	0.000	0.000	0.000	0.000	0.000	0.000	0.000
52	0.000	0.000	0.000	0.000	0.000	0.000	0.000	0.000
53	0.000	0.000	0.000	0.000	0.000	0.000	0.000	0.000
54	0.000	0.000	0.000	0.000	0.000	0.000	0.000	0.000
55	0.000	0.000	0.000	0.000	0.000	0.000	0.000	0.000
56	0.000	0.000	0.000	0.000	0.000	0.000	0.000	0.000
57	0.000	0.000	0.005	0.000	0.000	0.000	0.000	0.000

LIST OF REFERENCES

LIST OF REFERENCES

Allanson, B.R. 1973. The fine structure of the periphyton of Chara sp. and its significance to the macrophyte-periphyton metabolic model of R.G. Wetzel and H.L. Allen. Freshwat. Biol. 3:535-542.

Barko, J.W. and R.M. Smart. 1981. Comparative influences of light and temperature on the growth and metabolism of selected submersed freshwater macrophytes. Ecol. Monogr. 51:219-235.

Barko, J.W. 1982. Influence of potassium sources (sediment vs. open water) and sediment composition on the growth and nutrition of a submersed freshwater macrophyte (Hydrilla verticillata (L.f.) Royle). Aquat. Bot. 12:157-172.

BMDP 1982. BMDP2R, Stepwise regression. In: Dixon, W.J. (ed.) BMDP Statistical Software, 1981.

Daley, R.J. 1973. Experimental characterization of lacustrine chlorophyll diagenesis. II. Bacterial, viral and Herbivore grazing effects. Arch. Hydrobiol. 72:409-439.

Eminson, D. and G.L. Phillips. 1978. A laboratory experiment to examine the effects of nutrient enrichment on macrophyte and epiphyte growth. Verh. Internat. Verein. Limnol. 20:82-87.

Fukshansky, L. 1982. Optical properties of plants. In: Macfadyen, A. and E.D. Ford (eds.) Advances in Ecological Research, Vol. 12. pp. 21-40. Academic Press, London.

Govindjee and B.J. 1974. Light absorption, emission and photosynthesis. In: Stewart, W.D.P. (ed.) Algal Physiology and Biochemistry. pp.346-390. University of California Press, Berkeley.

Hutchinson, G. E. 1957. A Treatise on Limnolgy. I. Georgraphy, Physics and Chemistry. Wiley, New York. 1015 pp.

Jupp, B.P. and D.H.N. Spence. 1977. Limitations on macrophytes in a eutrophic lake, Loch Leven. I. Effects of phytoplankton. J. Ecol. 65:175-186.

Kavanagh, F. 1972. Photometric assaying. In: Kavanagh, F. (ed.) Analytical Microbiology. pp.44-121. Academic Press, New York.

Koch, A.L. 1970. Turbidity measurements of bacterial cultures in some available commercial instruments. Anal. Biochem. 38:252-259.

Kowalczewski, A. 1975. Periphyton primary production in the zone of submerged vegetation of Mikolajskie Lake. Ekol. Pol. 23:509-543.

Mendelssohn, I.A., K.L. McKee and W.H. Patrick, Jr. 1981. Oxygen deficiency in Spartina alterniflora roots: Metabolic adaptation to anoxia. Science 214:439-441.

Morgan, N.C. 1970. Changes in the fauna and flora of a nutrient enriched lake. Hydrobiologia 35:545-553.

Moss, B. 1976. The effects of fertilization and fish on community structure and biomass of aquatic macrophytes and epiphytic algal populations: An ecosystem experiment. J. Ecol. 64:313-342.

Mulligan, H.F. and A. Baranowski. 1969. Growth of phytoplankton and vascular aquatic plants at different nutrient levels. Verh. Internat. Verein. Limnol. 17:802-810.

Osborne, P.L. and B. Moss. 1977. Paleolimnology and trends in the phosphorus and iron budgets of an old man-made lake, Barton Broad, Norfolk. Freshwat. Biol., 7:213-233.

Phillips, G.L., D. Eminson, and B. Moss. 1978. A mechanism to account for macrophyte decline in progressively eutrophicated freshwaters. Aquat. Bot. 4:103-126.

Sand-Jensen, K. 1977. Effect of epiphytes on eelgrass photosynthesis. Aquat. Bot. 3:55-63.

Sand-Jensen, K. and M. Søndergaard. 1981. Phytoplankton and epiphyte development and their shading effect on submerged macrophytes in lakes of different nutrient status. Int. Revue ges. Hydrobiol. 66:529-552.

Spence, D.H.N. 1976. Light and plant response in fresh water. In: Evans, G.C., R. Brainbridge and O. Radkham (eds.) Light as an Ecological Factor: II. pp.93-123. Blackwell Scientific Publications, Oxford.

Spence, D.H.N. 1981. Light quality and plant responses under water. In: Smith, H. (ed.) Light and the Daylight Spectrum. pp. 245-275. Academic Press, London.

Spence, D.H.N. 1982. The zonation of plants in freshwater lakes. In: Macfadyen, A. and E.D. Ford (eds.) Advances in Ecological Research, Vol. 12. pp.37-126. Academic Press, London.

Søndergaard, M. 1981. Kinetics of extracellular release of ^{14}C-labelled organic carbon by submerged macrophytes. Oikos 36:331-347.

Van, T.K., W.T. Haller and G. Bowes. 1976. Comparison of the photosynthetic characteristics of three submersed aquatic plants. Plant Physiol. 58:761-768.

Van, T.K., W.T. Haller, G. Bowes and L.A. Garrard. 1977. Effects of light quality on growth and chlorophyll composition in Hydrilla verticillata, an aquatic weed in Florida. Hyacinth Control J. 15:29-31.

Wetzel, R. G. 1983. Limnology. 2nd ed., Saunders College Publishing, Philadelphia. 860 pp.

Wetzel, R.G., E.S. Brammer and C. Forsberg. 1983. Photosynthesis of submersed macrophytes in acidified lakes. I. Carbon fluxes and recycling of CO_2 in Juncus bulbosus L. Aquat. Bot. (Submitted)

White, W. Sedgefield. 1974. Role of calcium carbonate precipitation in lake metabolism. Ph.D. Thesis, Michigan State University. 141 pp.

Whittingham, C.P. 1976. Function in photosynthesis. In: Goodwin, T.W. (ed.) Chemistry and Biochemistry of Plant Pigments. pp. 624-654. Academic Press, New York.

General References

Butler, W. L. 1964. Absorption spectroscopy in vivo: Theory and application. Ann. Rev. Plant Physiol. 15:451-470.